Proceedings of the Korean Nuclear Society Spring Meeting
Seoul, Korea, May 1998

An Extended Numerical Calibration Method for an Electrochemical Probe in Thin Wavy Flow with Large Amplitude Waves

Ki Yong Choi and Hee Cheon NO

Dept. of Nuclear Eng., Korea Advanced Institute of Science and Technology,
373-1 Ku-song Dong, Yu-song Gu, Taejon 305-701, Korea

Abstract

The calibrating method for an electrochemical probe, neglecting the effect of the normal velocity on the mass transport, can cause large errors when applied to the measurement of wall shear rates in thin wavy flow with large amplitude waves. An extended calibrating method is developed to consider the contributions of the normal velocity. The inclusion of the turbulence-induced normal velocity term is found to have a negligible effect on the mass transfer coefficient. The contribution of the wave-induced normal velocity can be classified on the dimensionless parameter, V. If V is above a critical value of V, V_{crit}, the effects of the wave-induced normal velocity become larger with an increase in V. While its effects negligible for $V < V_{crit}$. The unknown shear rate is numerically determined by solving the 2-D mass transport equation inversely. The present inverse method can predict the unknown shear rate more accurately in thin wavy flow with large amplitude waves than the previous method.

1 Introduction

An electrochemical probe, developed by Reiss & Hanratty (1962) and Reiss & Hanratty (1963), is the most promising technique to measure the liquid-to-wall shear stress in two-phase flow, because it does not disturb the flow field near wall. In principle, it can be calibrated analytically and both the average value and the local value of the mass transfer rate or shear stress at a liquid-wall interface can be measured. This method has been used extensively in various geometrical systems by many investigators: Mitchell & Hanratty (1966), Sutey & Knudsen (1969), Nakoryakov et al. (1981), and etc. Mao & Hanratty (1991a) analyzed the performance of the electrochemical probe in the presence of large amplitude unsteady flows. It was found that the use of the quasi-steady solution to interpret the measured mass transfer rates would cause severe errors in the measurement of wall shear stress for large amplitude unsteady flows. However, the 2-D mass transport equation governing the calibrating rule of the electrochemical probe has been solved neglecting the normal convective term. Levich (1962) found that the normal convective term is of the same order with the axial convective term grounded on the order of magnitude analysis. In particular, the contribution of the normal velocity component to the mass transfer rates cannot be easily neglected for thin wavy flows with large wave heights. Therefore, the two-dimensional mass transport equation having a normal convective term needs to be considered as a governing equation. In this study, the effects of normal convective term on the mass transfer rates are numerically investigated. The numerical calibrating method, which can be applicable to unsteady thin wavy flow with large amplitude waves is developed.

2 Modelling of fluctuating velocity terms

A two-dimensional convective mass transport equation is written by

$$\frac{\partial C}{\partial t} + u\frac{\partial C}{\partial x} + v\frac{\partial C}{\partial y} = D(\frac{\partial^2 C}{\partial x^2} + \frac{\partial^2 C}{\partial y^2}). \tag{1}$$

The velocity components in the x and y directions are described by superposition of the wave-induced velocity fluctuation and the background turbulence. Thus, the instantaneous velocities are written by

$$u(x,y,t) = \overline{U}(x,y) + u'(y,t) + \tilde{u}(y,t), \tag{2}$$

$$v(x,y,t) = \overline{V}(x,y) + v'(y,t) + \tilde{v}(y,t), \tag{3}$$

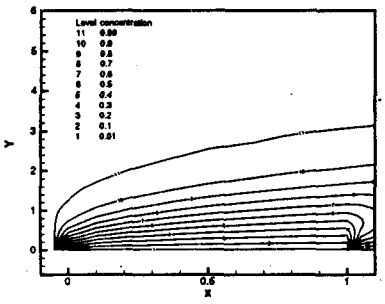

Figure 1 Calculated concentration profile for the case of $f^* = 0.1$ and $\hat{s} = 0.9$

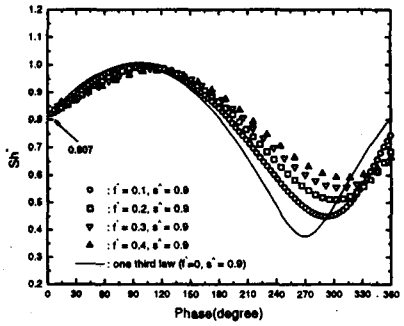

Figure 2 Frequency responses of Sh^* with the variation of f^*

where $\overline{U}$ and $\overline{V}$ represent the time-averaged velocities, u' and v' turbulent velocity fluctuations, and $\tilde{u}$ and $\tilde{v}$ wave-induced velocity fluctuations in x and y direction, respectively. It is assumed that the turbulent and wave-induced velocity fluctuations are statistically independent variables. The time-averaged values of the turbulent velocity fluctuations are assumed to be zero. When the flow is fully developed hydrodynamically and the measuring electrode is very small compared with the dimension of the channel, the x dependency of $u(x,y,t)$ can be neglected. Within so thin mass concentration boundary layer, the streamwise velocity is linear with y. Then Eq.(2) can be written by

$$u(y,t) = s(t)y = [\overline{S} + \frac{u_{rms}(y)}{\overline{U}(y)} \cdot \overline{S} \cdot F(t) + \tilde{s}(t)] \cdot y, \tag{4}$$

where $\overline{S}$ is the average shear rate defined by $\overline{S} = \overline{U}(y)/y$, and $\tilde{s}(t)$ is the wave-induced instantaneous shear rate defined by $\tilde{s}(t) = \tilde{u}(y,t)/y$. For the turbulence-induced normal fluctuating velocity component, v', v_{rms}/u^* is found to be quadratic function of y^+ close to a wall. Since the distribution of $v'(t)$ is much symmetric than $u'(t)$ and closer to Gaussian(Kreplin & Eckelmann (1979)), $v'(t)$ can be also represented by its root-mean-square value multiplied by random variable function $v'(y,t) = v_{rms}(y)F(t)$. As the fluctuating velocity components u' and v' are poorly correlated(Eckelmann (1974), Kim et al. (1987)) u' and v' can be treated independent of each other in the vicinity of the wall. For the wave-induced normal velocity fluctuation, $\tilde{v}(y,t)$, Akai et al. (1977) found that the velocity fluctuation in wavy water film flow greatly depends on the interfacial waves, especially, its periodity, and the wave effect depth is nearly equal to one wave height. Therefore, for thin water film flows, the normal velocity fluctuation highly depends on the interfacial normal wave velocity. When a linear variation of the wave-induced normal velocity with respect to the water film thickness is assumed, a wave-induced normal velocity fluctuation, $\tilde{v}(y,t)$, can be expressed $\tilde{v}(y,t) \cong \frac{y}{\delta} v_i(t)$. It is rather simple but reasonable approximation when the boundary conditions are considered both at the wall($y = 0$) and interface($y = \overline{\delta}$). The normal velocity thus can be rewritten as follows:

$$v(y,t) = v_{rms}F(t) + \frac{y}{\overline{\delta}} v_i(t). \tag{5}$$

3 Numerical methods

3.1 Direct Problem

For a given shear rate, $s(t)$, Eq.(1) is numerically solved to give the concentration gradient at the surface along the electrode. This problem is called a "direct problem" by Mao & Hanratty (1991a). Eq.(1) can be written in a dimensionless form using Eq.(4) and Eq.(5) as

$$\frac{\partial C^+}{\partial \tau} + S^+(\tau) Y \frac{\partial C^+}{\partial X} + Sc^{2/3} L^{+1/3} v^+ \frac{\partial C^+}{\partial Y} = \frac{\partial^2 C^+}{\partial Y^2}. \tag{6}$$

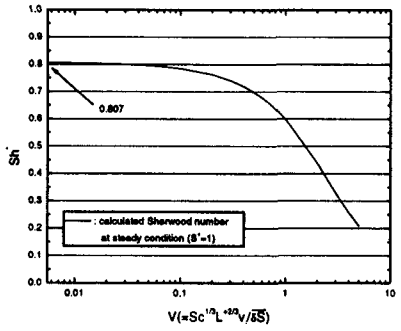

Figure 3 Effects of V on Sh^* at steady condition

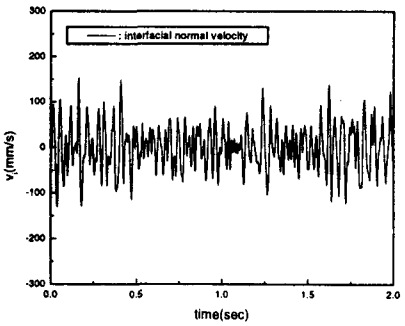

Figure 4 The calculated time series of v_i

If Eq.(5) is plugged into the normal convective term of Eq.(6), the third term in the left hand side of Eq.(6) can be rewritten by

$$Sc^{2/3}L^{+1/3}v^{+}\frac{\partial C^{+}}{\partial Y} = Sc^{2/3}L^{+1/3}v^{+}_{rms}F(t)\frac{\partial C^{+}}{\partial Y} + \frac{YV}{S^{+}(\tau)}\frac{\partial C^{+}}{\partial Y}, \tag{7}$$

where, dimensionless normal interfacial velocity V is defined by $V = Sc^{1/3}L^{+2/3}v_i/\overline{\delta S}$. For the schematic diagram of the control volume and more detailed information of the calculation domain, refer to the figures 1 and 2 in the paper by Mao & Hanratty (1991a). When the convective term is treated with an upwind scheme and the piecewise linear concentration profile is assumed, the following finite difference equation is obtained

$$A_p(i,j)C^{n+1}_{i,j} - A_u(i,j)C^{n+1}_{i,j+1} - A_d(i,j)C^{n+1}_{i,j-1} - A_l(i,j)C^{n+1}_{i-1,j} = C^{n}_{i,j}, \tag{8}$$

where

$$A_u(i,j) = \frac{\Delta\tau}{\delta Y_{j+1}\Delta Y_j} - \frac{\Delta\tau Sc^{2/3}L^{+1/3}v^{+}_{rms}F(t)}{\delta Y_j + \delta Y_{j+1}} - \frac{\Delta\tau Y_j V}{S^{+n}(\delta Y_j + \delta Y_{j+1})}, \tag{9}$$

$$A_d(i,j) = \frac{\Delta\tau}{\delta Y_j\Delta Y_j} + \frac{\Delta\tau Sc^{2/3}L^{+1/3}v^{+n}}{\delta Y_j + \delta Y_{j+1}} + \frac{\Delta\tau Y_j V}{S^{+n}(\delta Y_j + \delta Y_{j+1})}, \tag{10}$$

$$A_l(i,j) = S^{+n}\Delta\tau Y_j/\delta X_i, \tag{11}$$

$$A_p(i,j) = A_u(i,j) + A_d(i,j) + A_l(i,j) + 1. \tag{12}$$

Here, the second and third terms of the right hand sides in Eq.(9) and Eq.(10) is the contributions due to the turbulence-induced and the wave-induced normal velocities, respectively. For each time step, the concentration field is calculated by solving a penta-diagonal matrix with SOR method. Modified Sherwood number Sh^* can be calculated by means of the integration of the concentration gradient at the electrode surface. For steady flow the modified Sherwood number becomes 0.807. Typical result of the calculated mass concentration profile is plotted in Figure 1. The development of the mass concentration boundary layer can be observed. At the right edge of the electrode $X = 1$, the thickness of the mass concentration boundary layer is approximately $Y = 3$, which corresponds to $y^{+} = 0.4$. It indicates that the thickness of the mass concentration boundary layer is confined within very thin region.

3.2 Inverse problem

A problem to find out the unknown shear rate based on the measured mass transfer coefficient is called as "inverse problem" by Mao & Hanratty (1991a). If the time step, $\Delta\tau_k$ is assumed to be very small, the shear rate at time τ_{k+1} can be written by

$$S^{+}_{k+1} \cong S^{+}_{k} + (Sh^{*}_{k+1} - Sh^{*}_{k})\frac{\epsilon S^{+}_{k}}{Sh^{*}[(1+\epsilon)S^{+}_{k}] - Sh^{*}[S^{+}_{k}]}, \tag{13}$$

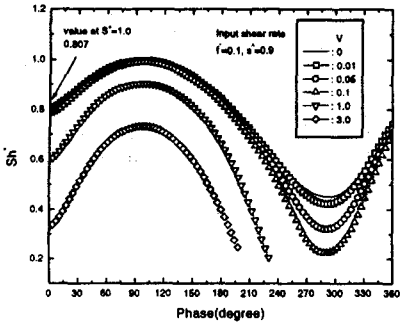

Figure 5 Frequency responses of Sh^* according to the variation of V

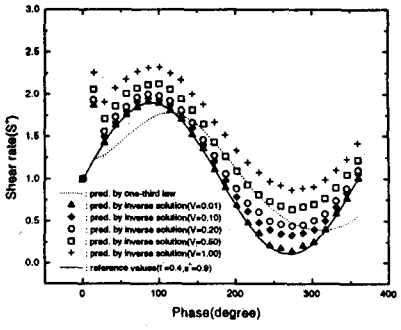

Figure 6 Predictions of the shear rate S^+ by the inverse method

where ϵ is a perturbation factor. The term $Sh^*[S_k^+]$ can be replaced with the measured value of Sh_k^* due to the first assumption, but $Sh^*[S_{k+1}^+]$ is obtained by solving the direct problem once for a given $(1+\epsilon)S_k^+$. S_{k+1}^+ is adjusted until the calculated modified Sherwood number at τ_{k+1} is reasonably close to the measured Sh_{k+1}^*.

4 Results and Discussion

4.1 Direct problem without the normal convective term

To investigate the frequency responses of the mass transfer rates and the effects of the large amplitude variations of the shear rate, Eq.(6) is solved numerically by assuming a sinusoidal variation of the shear rate, that is,

$$S^+(n) = 1 + \hat{s}\sin(2\pi f^* n d\tau), \tag{14}$$

where $\hat{s}$ is the fluctuating amplitude of the shear rate and f^* is the dimensionless frequency. The fluctuating amplitude of the shear rate and the frequency are varied to study their effects on the mass transfer coefficient, respectively. The calculated mass transfer rates are converted to the modified Sherwood number using the concentration gradient at the wall. From scaling analysis, the dimensionless frequency f^* of 0.1 corresponds to the real frequency of 1Hz or 5Hz. It has been reported that the dominant frequency for wavy two-phase flow lies around 10Hz (Chu & Dukler (1974), Takahama & Kato (1980), Brauner & Maron (1982), Brauner & Maron (1983)). Therefore, the variation of the dimensionless frequency f^* from 0.1 to 0.4 can be assumed to be reasonable to simulate the wavy two-phase flow. Figure 2 shows the typical results when the frequency f^* is varied from 0.1 to 0.4 for $\hat{s} = 0.9$. As shown in Figure 2, the calculated Sh^* at the initial time step becomes 0.807 as predicted by the steady solution. As predicted in literature, the calculated Sh^* shows the time lag with respect to the steady solution. High frequency results in both the phase shift and the decrease of the amplitude in Sherwood number. As the frequency increases, the phase shift increases and the amplitude in Sherwood number decreases. It indicates that the quasi-steady state solution, i.e., one-third power law, is not valid for flow with shear rates of high frequencies. The present result is well consistent with those by the previous workers(Mao & Hanratty (1991a), Mao & Hanratty (1991b)).

4.2 Direct problem with the normal convective terms

4.2.1 Effects of turbulent-induced fluctuations

The normal velocity is considered by its root-mean-square value multiplied by random variable function. The reported maximum value of the proportional constant of 0.009 is selected to investigate the effects on the modified Sherwood number conservatively. The effect of the turbulence-induced normal velocity is found to be negligible even though the maximum proportional constant is used. It is attributed to the facts that the rms value of the turbulence-induced fluctuating normal velocity is very close to zero because the mass transfer boundary layer is very thin and the calculation domain is confined within such a thin layer.

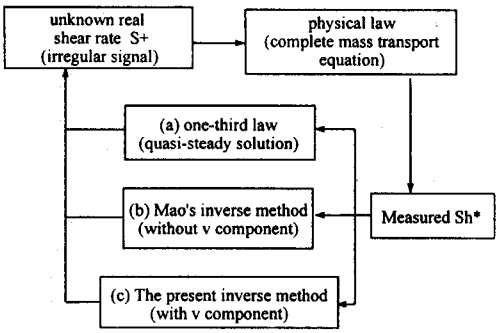

Figure 7 Schematic block diagram for prediction of the unknown shear rate through the inverse methods

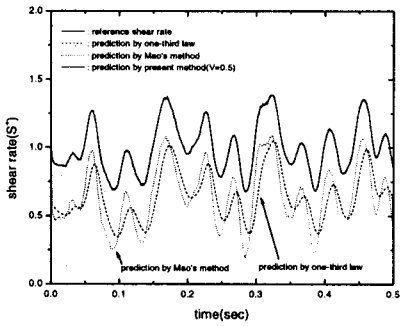

Figure 8 Predictions of the present inverse method($V = 0.5$)

4.2.2 Effects of wave-induced fluctuations

The effects of the dimensionless normal interfacial velocity, V on Sh^* are investigated at a fixed shear rate of $S^+ = 1$. As shown in Figure 3, Sh^* approaches to 0.807 as V decreases. When V is greater than approximately 0.1, Sh^* starts to drop rapidly. Therefore, the steady solution of needs to be modified for V greater than $V_{crit} = 0.1$. For the interfacial normal velocity, one of the local liquid film thickness data which are obtained in the condition of cocurrent air-water stratified flow is used as reference data. It is obtained at the liquid and the air velocities of $u_f = 0.97m/s$ and $u_g = 8.8m/s$, in the condition of large amplitude wave region. Based on the reference film thickness data, v_i is calculated from the relation by (Kang & Kim (1993)). The obtained v_i fluctuates with a large amplitude as can be seen in Figure 4. The estimated root-mean-value of v_i is roughly the order of $0.1m/s$. It can be thus inferred that v_i has the value of about 10^{-1} for the large amplitude wavy region. From the order of the magnitude of the variables consisting of V, it can be inferred that V has a value close to V_{crit}. When the similar estimation for V is performed for data from the smooth and 2-D wavy regimes, it is found to be smaller than V_{crit}. When the wave-induced normal velocity is included into the 2-D transport equation, the frequency effects are investigated. The results for $f^* = 0.1$ and $\hat{s} = 0.9$ are plotted in Figure 5. A large decrease in Sh^* around $\theta = 300^o$ can be observed compared with the result in the case of $V = 0$, though the initial values of Sh^* are almost the same to 0.807 up to $V = 0.1$. For the larger values than $V = 0.1$, not only the initial value of Sh^+ is reduced, but also the frequency response becomes greatly distorted.

4.3 Inverse problem with/without the normal convective term

When without the normal convective term, the modified Sherwood number, which was already calculated by the direct problem solver, is used as an input for the inverse problem. The solution of the inverse problem should be reasonably close to the sinusoidal shear rate which was used in the direct problem. The input shear rate is predicted with high accuracy. When the effect of the wave-induced normal velocity is considered, the magnitude of the wave-induced normal velocity is varied by the variation of the dimensionless normal interfacial velocity V. The effects of the turbulence-induced normal velocity fluctuations are ignored because their effects are found to be negligible in the previous section. The typical results are shown in Figure 6, where $f^* = 0.4$ and $\hat{s} = 0.9$ are used as a reference input shear rate. Compared with the results by the steady solution, it shows no time lag and good agreement with the reference values. As the magnitude of V increases, the deviation from the reference values appears. However, the agreement can be considered acceptable up to $V = 0.1$. It implies that the shear rate cannot be well predicted for $V > V_{crit}$ even if the inverse method is used.

4.4 Applications

The schematic block diagram for the logic to predict the unknown shear rate is shown in Figure 7. As shown in Figure 7, there are three kinds of inverse solvers to predict the unknown shear rate: one-third law, Mao & Hanratty (1991b)'s method, the present method. The weakness of Mao & Hanratty (1991b)'s approach is

that they solved an incomplete governing equation inversely, neglecting the effects of the normal velocity on Sh^*. If the measured Sh^* highly depends on the normal velocity, their prediction cannot predict the original shear rate because it does not consider the effects of the normal velocity. In the present work, a total of 1,000 points are normalized with their average value to simulate the dimensionless shear rate, which are obtained by sampling the local liquid film thickness at a sampling rate of 50Hz (Choi & NO (1997)). The parameter describing the effects of the normal velocity, V is assumed to have a value of 0.5 to simulate the large amplitude wave flow. Comparison of the predictions by the present inverse method with those by other methods is shown in Figure 8. As can be seen in Figure 8, the present inverse solver reconstructs the original shear rate very well. As expected, the predictions by the one-third law result in the phase shift and poor agreement with the original shear rate. The predictions by the inverse method suggested by Mao & Hanratty (1991b) show better agreement than those by the one-third law. However, it shows poor predictions than the present inverse solver does. When the large amplitude waves exists and the thickness of the liquid film is thin, the normal velocity component makes large contribution to the mass transfer coefficient. Therefore, neglecting its contribution results in the poor prediction of the shear rate. It is noteworthy that the present inverse method is based on the assumption of the linear relationship between the normal interfacial velocity and the wave-induced normal velocity. Up to now, there is no available information to verify the assumption. Therefore, the absolute value of V in itself does not have any particular physical meaning. However, it is clear from the present work that the prediction method of the unknown shear rate should consider the contribution of the wave-induced normal velocity when applied to the large amplitude wave region.

5 Conclusions and Recommendations

The magnitude of the wavy effect on the fluctuating normal velocity is expressed using the dimensionless variable V. It is shown that the inclusion of the turbulence-induced fluctuating component into the 2-D mass transport equation has negligible effects on the mass transfer coefficient. However, the wave-induced normal velocity cannot be ignored and the modified Sherwood number highly depends on V when $V > V_{crit}$. An extended inverse method to predict the shear rate in large amplitude wavy flow is suggested. It is found that the neglect of the contribution of the wave-induced normal velocity can cause a large error to predict the shear rate. The present numerical tools are applicable to large amplitude wave flow as calibration relation between the measured mass transfer coefficient and the wall shear rate. It is recommended that the more detailed study on the normal velocity in the thin wavy flow needs to be performed experimentally or theoretically to validate the present results.

References

[1] Akai, M., Inoue, A., & Aoki, S., 1977 *Theor. Appl. Mech.* **25**, 445–456.
[2] Brauner, N. & Maron, D. M., 1982 *Int. J. Heat Mass Transfer* **25**, 99–110.
[3]Brauner, N. & Maron, D. M., 1983 *Chem. Eng. Sci.* **38**, 775–788.
[4] Choi, K. Y. & NO, H. C., 1997 *submitted to Int. J. Multiphase Flow.*
[5] Chu, K. J. & Dukler, A. E., 1974 *AIChE J.* **20**, 695–706.
[6] Eckelmann, H., 1974 *J. Fluid Mech.* **65**, 439–459.
[7] Kang, H. C. & Kim, M. H., 1993 *Int. J. Multiphase Flow* **19**, 35–49.
[8] Kim, J., Moin, P., & Moser, R., 1987 *J. Fluid Mech.* **177**, 133–166.
[9] Kreplin, H. P. & Eckelmann, H., 1979 *Phys. Fluids* **22**, 1233–1239.
[10] Levich, V. G., 1962 *Physicochemical hydrodynamics.* Prentice Hall, Englewood Cliffs, NJ.
[11] Mao, Z. & Hanratty, T. J., 1991a *Int. J. Heat Mass Transfer* **34**, 281–290.
[12] Mao, Z. & Hanratty, T. J., 1991b *Experiments in Fluids* **11**, 65–73.
[13] Mitchell, J. E. & Hanratty, T. J., 1966 *J. Fluid Mech.* **26**, 199–221.
[14] Nakoryakov, V. E., Kashinsky, O. N., Burdukov, A. P., & Odnoral, V. P., 1981 *Int. J. Multiphase Flow* **7**, 63–81.
[15] Reiss, L. P. & Hanratty, T. J., 1962 *AIChE J.* **8**, 245–247.
[16] Reiss, L. P. & Hanratty, T. J., 1963 *AIChE J.* **9**, 154–160.
[17] Sutey, A. M. & Knudsen, J. G., 1969 *AIChE J.* **15**, 719–726.
[18] Takahama, H. & Kato, S., 1980 *Int. J. Multiphase Flow* **6**, 203–215.